Biometals
DOI 10.1007/s10534-012-9561-7

Changes in morphology, cell wall composition and soluble proteome in *Rhodobacter sphaeroides* cells exposed to chromate

Francesca Italiano · Sara Rinalducci · Angela Agostiano · Lello Zolla · Francesca De Leo · Luigi R. Ceci · Massimo Trotta

Received: 13 March 2012 / Accepted: 17 May 2012

Abstract The response of the carotenoidless *Rhodobacter sphaeroides* mutant R26 to chromate stress under photosynthetic conditions is investigated by biochemical and spectroscopic measurements, proteomic analysis and cell imaging. Cell cultures were found able to reduce chromate within 3–4 days. Chromate induces marked changes in the cellular dimension and morphology, as revealed by atomic force microscopy, along with compositional changes in the cell wall revealed by infrared spectroscopy. These effects are accompanied by significant changes in the level of several proteins: 15 proteins were found up-regulated and 15 down-regulated. The protein content found in chromate exposed cells is in good agreement with the biochemical, spectroscopic and microscopic results. Moreover at the present stage no specific chromate-reductase could be found in the soluble proteome, indicating that detoxification of the pollutant proceeds via aspecific reductants.

Keywords Chromate reduction · Photosynthesis · *Rhodobacter sphaeroides* · Two-dimensional gel electrophoresis · Atomic force microscopy · Attenuated total reflection-fourier transformed infra red spectroscopy

Introduction

Chromium is a widespread pollutant introduced in the environment as waste or by-product of industrial activities (Barceloux 1999). Its most stable and common chemical forms found in the environment are the trivalent and hexavalent species, which differ significantly in their physico-chemical properties and biological toxicity responsiveness (Katz and Salem 1993). The most common form of Cr(VI) is the chromate oxyanion (CrO_4^{2-}), a highly water soluble compound that can cross cellular membranes (Cervantes et al. 2001) and is toxic for most organisms. Chronic exposure may lead to mutagenesis and carcinogenesis arising from the formation of reactive oxygen intermediates generated during the intracellular reduction to the less toxic Cr^{3+} (Cervantes et al. 2001). Trivalent

Electronic supplementary material The online version of this article (doi:10.1007/s10534-012-9561-7) contains supplementary material, which is available to authorized users.

F. Italiano · A. Agostiano · M. Trotta (✉)
CNR-IPCF, Consiglio Nazionale delle Ricerche, Istituto per i Processi Chimico Fisici, Via Orabona 4, 70125 Bari, Italy
e-mail: m.trotta@ba.ipcf.cnr.it

S. Rinalducci · L. Zolla
Dipartimento di Scienze Ecologiche e Biologiche (DEB), Università della Tuscia, Viterbo, Italy

A. Agostiano
Dipartimento di Chimica, Università di Bari, Bari, Italy

F. De Leo · L. R. Ceci
Istituto di Biomembrane e Bioenergetica (CNR), Bari, Italy

Published online: 04 June 2012

chromium Cr^{3+} forms poorly water soluble compounds and is toxic to a minor extent although it was shown to cause DNA damage and to inhibit the activity of DNA topoisomerase in bacteria (Plaper et al. 2002).

Several microorganisms exposed to chromate have shown resistance mechanisms that include biosorption, diminished intracellular accumulation by obstruction of the uptake system or active chromate efflux, extracellular precipitation and, aerobic and/or anaerobic reduction (Ramirez-Diaz et al. 2008; Cheung and Gu 2007; Cervantes et al. 2001; McLean et al. 2000; Ackerley et al. 2004; Morais et al. 2011). The most intriguing is the reduction of chromate to the trivalent cation, a detoxification mechanism that has been proposed as potential remediation strategy for contaminated sites in alternative to expensive physicochemical means (Cervantes et al. 2001; Cheung and Gu 2007). Among microorganisms, photosynthetic ones have been investigated for their potential application in remediation strategy and the gram-negative, purple non-sulfur bacterium *Rhodobacter* (*R.*) *sphaeroides* has shown promising possibilities having a remarkable ability to grow under aerobic respiration, anoxygenic photosynthesis, and anaerobic respiration (Kiley and Kaplan 1988; Schultz and Weaver 1982). Strain R26 is a stable deletion mutant susceptible to photooxidative damage due to the absence of photoprotective carotenoid pigments (Sistrom et al. 1956), known for its ability to tolerate high concentrations of several heavy metal ions (Giotta et al. 2006), to bioaccumulate nickel and cobalt (Buccolieri et al. 2006; Italiano et al. 2009; Italiano et al. 2011) and to reduce oxyanions as tellurite and selenite (Borsetti et al. 2003). The present paper investigates the response of *R. sphaeroides* R26 to chromate stress under photosynthetic conditions through combination of proteomics, Attenuated Total Reflectance-Fourier Transform Infrared Spectroscopy (ATR-FTIR) and Atomic Force Microscopy (AFM) investigations.

Materials and methods

Chemicals

Chemicals for bacterial cell culture, PMSF (phenylmethanesulphonylfluoride), DNAse I (from bovine pancreas), RNAse A (from bovine pancreas Type II-A), methanol (≥99.8 %), acetone (≥99.5 %), tri *n*-butylphosphate (≥99 %), TRIS (tris(hydroxymethyl)aminomethane), Triton X-100, glycerol (ACS reagent, ≥99.5 %), *p*-dimethylaminobenzaldehyde (DMAB), glacial acetic acid, perchloric acid (70 %), poly-L-lysine (Mw = 70–100 kDa) and 5,5′-dithiobis(2-nitrobenzoic acid) (DTNB) were obtained from Sigma-Aldrich. Urea, thiourea, CHAPS, DTT (dithiothreitol), IPG (Immobilized pH Gradient) buffer pH 3–10 and 4–7, SDS (sodium dodecylsulphate), iodoacetamide and IPG strips (13 cm, pH ranges: 3–10 or 4–7) were purchased from GE-Healthcare. Mica slides were purchased from NanoAndMore GmbH (Wetzlar, Germany).

Bacterial strain and growth conditions

Rhodobacter sphaeroides R26 was grown in light under anaerobic conditions according to Buccolieri et al. (2006). Medium 27 of the German Collection of Microorganisms and Cell Cultures (http://www.dsmz.de/) was used as control or added with Na_2CrO_4 from a stock solution by microfiltration (0.22 µm filters PES Filter Media, Whatman) to a final concentration of 0.2 mM.

Cr(VI) effect on photosynthetic growth and time-course Cr(VI) reduction

The photosynthetic growth was monitored at 535 nm as previously illustrated (Giotta et al. 2006). The cultures illumination was achieved by 100-watt tungsten filament light bulbs placed at 25 cm from the vessels (120 µE m^{-2} s^{-1}).

Anaerobic cultures were periodically used to determine cell density and extent of chromate reduction. Cell-free control was prepared to monitor whether abiotic reduction occurred and negligible contribution of broth components was found. All experiments were done in duplicate.

Chromate reduction was monitored by determining its residual concentration in the growth medium with time at 540 nm after reaction with 1,5-diphenylcarbazide in acid solution (Lovley and Phillips 1994).

Localization of reductase activity

One liter of control growth in late exponential growing phase was centrifuged at 14,000 × *g* at 4 °C for 15 min. Harvested cells were washed in 20 mM Tris–HCl pH 8 and re-suspended in the same buffer containing

100 μg ml^{-1} DNase I and 0.1 mM PMSF and lysed in a French pressure cell at 1.38 × 10^8 Pa and the homogenate was centrifuged at 16,000×*g* at 4 °C for 15 min to remove debris and intact cells. The supernatant was centrifuged at 150,000×*g* for 2 h to separate the membrane fraction from the soluble fraction. Cell fractions were separately assayed for chromate reduction at 37 °C by following the decrease in time of CrO_4^{2-} in the assay mixture containing the cell fraction, 20 mM Tris–HCl at pH 7.0, 0.2 mM sodium chromate. The membrane fraction was subject to three washing to minimize possible contaminations. Control experiments on thermally inactivated cell fractions were performed after heating for 5 min at 100 °C.

Chromate reduction data were normalized against protein concentration measured by bicinchoninic acid assay (Smith et al. 1985) using bovine serum albumin (BSA) as standard.

Reduced thiols (RSH) determination

The concentration of RSH was measured by Ellman's reagent or DTNB according the previously published protocol (Turner et al. 1999). Cells in late exponential growing phase were harvested by centrifugation at 14,000×*g* at 4 °C for 5 min from 1 l of control or chromate-enriched cultures. The pellets were resuspended by vortexing in 1 ml of a freshly prepared solution of 50 mM Tris–HCl pH 8.0, 5 mM EDTA, 0.1 % SDS and 0.1 mM DTNB, incubated at 37 °C for 30 min, briefly vortexed and centrifuged at 15,000×*g* for 10 min. The absorbance at 412 nm of the supernatant of each fraction was recorded zeroing against the sole reagent buffer and using the extinction coefficient of oxidized DTNB of 1.36 × 104 M^{-1} cm^{-1}. RSH concentrations were normalized against protein concentration measured by bicinchoninic acid assay (Smith et al. 1985) using BSA as the standard. All experiments were performed at least in three independent replicates.

AFM analysis

Mica slides as substrate for AFM of bacteria were pretreated with poly-L-lysine to ensure cell adhesion as in literature (Schaer-Zammaretti and Ubbink 2003). Slides were soaked and stored in a 0.1 % w/v poly-L-lysine solution for at least 12 h. 10 μl of bacterial suspension (10^8 CFU/ml) in late exponential growing phase were deposited on treated slides, let dry at room temperature, rinsed with distilled water, dried again and finally mounted for imaging. All experiments were performed in tapping mode by using a PSIA XE-100 atomic force microscope equipped with a standard 125 μm long microlever with a force constant of 42 N/m and a resonant frequency of 320 kHz. Topographic and phase images were recorded simultaneously. Randomly selected cells (50 per treatment) were measured and analyzed. Roughness analyses were also performed on samples, conducted according to the manufacturer's software program XEI (PSIA Corp., version 1.7.3) using the cross section profiles, i.e. the profiles of the height of the cell measured along the two dimensions of the cell. The root-mean-square (RMS) average of the surface roughness value was calculated as the standard deviation of all the height values within the given area.

ATR-FTIR measurements

ATR-FTIR mid-infrared spectra of cell suspensions in late exponential growing phase were acquired with a VARIAN 670-IR spectrometer equipped with an ATR horizontal sampling apparatus. The internal reflection element (IRE) was a diamond microprism mounted into a stainless steel plate. All spectra were recorded at room temperature in the region of 4,000–600 cm^{-1}, averaging 100 scans. Resolution was 2 cm^{-1}. Spectra from cells grown in presence of CrO_4^{2-} and in control media were recorded and the amide I band at 1648 ± 1 cm^{-1} was used as internal standard for normalizing absorbance.

Water soluble protein fraction extraction

The red-brown (roughly 30 ml) soluble fraction obtained with the above procedure from cells harvested after 50 and 220 h in control and chromate case respectively was precipitated with 14 vol of acetone–methanol–tri *n*-butylphosphate (12:1:1) overnight at 4 °C, as previously reported (Pisani et al. 2009). The pellet was collected by 20 min centrifugation (2,800×*g*, 4 °C), washed with 30 ml of tri *n*-butylphosphate, acetone, and methanol in this order and solubilized in 2.5 % CHAPS. Total protein content was determined according to the Bradford method

(Biorad Protein Assay) using BSA as standard. The CHAPS solution was then added with the rehydration buffer to a final protein concentration of 1.0–1.5 mg ml^{-1}.

Two dimensional gel electrophoresis

350 µg of proteins were loaded onto suitable linear IPG strip for electrophoretic separation. Isoelectrofocusing (IEF) was performed with a total Vh of 70.000 in 4–7 pH strips as described previously (Pisani et al. 2009). Strips from IEF were equilibrated for 15 min in Buffer I, then for other 15 min in Buffer II, and finally sealed to a 15 × 15 cm 10 % Polyacrylamide gel by 0.5 % Agarose in TGS buffer. Electrophoresis was performed at 18 °C using TGS as running buffer at 25 mA for 1 h and at 50 mA for 4 h. Gels were stained with Coomassie Colloidal G250 and destained with Milli Q water (Millipore).

Two dimensional gel electrophoresis was run on two sets of four independent batches of soluble protein fractions obtained from control and CrO_4^{2-} biomasses respectively. Gels were scanned with an Image Scanner (Amersham Biosciences) and analysed with the software Image Master 2D 6.0 Platinum (GE-Healthcare). Spots from the two sets were compared via *t*-student test and those found with a *t*-value higher than 7 were recovered from the gels and analyzed by tandem mass spectrometry (MS/MS).

MS/MS analysis

Protein spots were excised from stained gels and subjected to in-gel trypsin digestion as described (Pisani et al. 2009). The recovered peptide mixtures were separated by using a nanoflow-HPLC system (Ultimate, Switchos, Famos, LC Packings, Amsterdam, Netherlands) coupled with a High Capacity Ion Trap HCTplus (Bruker-Daltonik, Germany). Protein identification was performed by searching in the National Center for Biotechnology Information non-redundant database (NCBInr) by using the Mascot program (http://www.matrixscience.com). For positive identification, the score of the result had to be over the significance threshold ($P < 0.05$).

Results and discussion

Chromate effect on the photosynthetic growth

Chromate at a concentration of 0.2 mM causes a significant increase in the lag-phase duration of the photosynthetic growth of *R. sphaeroides*, while the population size at the stationary phase and the growth rate remain substantially unchanged (Fig. 1). Cell cultures completely reduced 0.2 mM chromate in the growth medium within 80–90 h from light exposure and the exponential growth phase started several hours after the complete chromate reduction (Fig. 1). To localise the chromate reductase activity, chromate reduction was checked on whole cells and on membrane and soluble fractions (see Fig. 2), and on the corresponding thermally inactivated controls. At the cellular concentration used, reduction is accomplished mostly by the soluble fraction in the hours time scale along with a minor contribution arising from extracellular components, while membrane fraction or whole cells are respectively much slower or ineffective on this time scale. Although care was taken in obtaining a clean membrane fraction preparation, we cannot exclude that some contamination from the soluble fraction may be responsible of at least part of the observed reducing activity. Control experiments on thermally inactivated cell fractions show that non specific and non enzymatic reductants contribute little to the chromate reduction. The fact that the largest contribution to chromate reduction arises from the soluble intracellular fraction strongly suggests that the oxyanion must be transported into the cytoplasm for being detoxified, presumably by using sulphate or phosphate transport systems as shown for several microorganisms and plants (Cervantes et al. 2001; Aguilar-Barajas et al. 2011). *Rhodobacter sphaeroides* genome contains the gene *ChrA* coding for a predicted protein annotated as chromate transporter (http://www.genome.jp/dbget-bin/www_bget?rsp:RSP_2282), as supported by the similarity with homologous gene identified in *Pseudomonas aeruginosa* (Pimentel et al. 2002). The actual CrO_4^{2-} concentration is probably small and its reduction is a rather slow process that requires the very long lag-phase found in the growth experiments. On this basis, chromate reducing activity appears constitutive rather than induced and the growth of the bacterium can only take place once chromate concentration has dropped below a non toxic lower limit. The

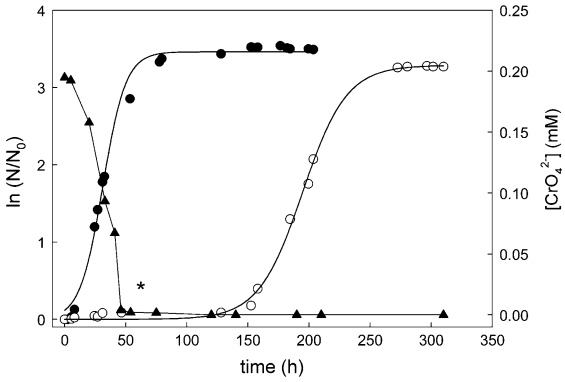

Fig. 1 Photosynthetic growth curves of *R. sphaeroides* R26 in control (*filled circles*) and 0.2 mM CrO_4^{2-} (*empty circles*) culture media. The time course of the chromate reduction during the growth of *R. sphaeroides* is also shown (*filled triangles*). The *asterisk* indicates the time point at which the cells have fully reduced chromate

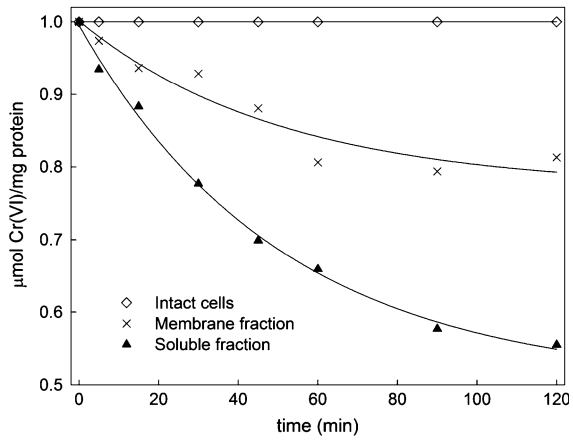

Fig. 2 Comparison of time course of Cr(VI) reduction in presence of intact cells, membrane fraction and soluble fraction of *R. sphaeroides* cells. Chromate concentration in membrane and soluble fractions decreases monoexponentially and the best fit represented by the *solid lines*

soluble fraction of a number of bacterial species shows chromate-reductase activity as in *Pseudomonas putida* MK1 (Park et al. 2000) and *Pseudomonas ambigua* G-1 (Suzuki et al. 1992) and such reduction can be performed by nonspecific soluble reductants, i.e. glutathione, glutathione reductase, cytochromes, cysteine, carbohydrates, NADH, NADPH, nucleotides, or ascorbic acid (Codd et al. 2003; Stearns et al. 1995). In agreement with this hypothesis several enzymes able to undergo redox reactions were found up-regulated in our proteomic data.

It is worthy to note that several authors have found a chromate reductase activity associated with the membrane fraction of cell extracts, as in the cases of anaerobically grown *Shewanella oneidensis* MR-1 (Myers et al. 2002) or *Enterobacter cloacae* cells (Wang et al. 1990). Our data do not rule out this possibility; indeed the reduction experiment performed on different cell fractions and on whole cells do not exclude that the cell wall is able to reduce chromate, but rather indicates that if such activity is present it takes place on much longer time scale. Furthermore the composition of the bacterial cell wall (teichoic acids, polycarbohydrates, and other diol-containing having reducing capability) and the possible activity of different cell wall-associated reductases, suggest that Cr(VI) can be partly reduced by the bacterial cell wall (Cervantes et al. 2001).

Chromate effect on cell morphology

Morphology and surface topology of control and chromate exposed bacterial cells were investigated by AFM (Fig. 3). Control cells were found having average length and width of 2.0 ± 0.6 and 1.2 ± 0.5 µm respectively (Fig. 3 panels a-1, a-2, c-1, and c-2). In presence of 0.2 mM CrO_4^{2-}, the average length and width of cells were found of 4.0 ± 1.0 and 0.8 ± 0.4 µm respectively (Fig. 3 panels b-1, b-2, d-1, and d-2). Moreover a significant increase in the cell height was found, passing from 120 ± 40 nm in control samples to 200 ± 40 nm in chromate samples (Fig. 3 panels c-3 and d-3). The relatively lower resolution of images from chromium treated cells is possibly due to a surface roughness increase, which seems to cause tip-sample interactions resulting in a negligible feedback. The offline analysis of AFM images and surface height profiles indicate a relatively smooth surface of control cells in contrast to chromium treated cells where structural alteration in the topography can be inferred (Fig. 3 panels c-3, d-3). Consistently with this finding, roughness analyses revealed that the surface of control cells was relatively homogeneous with R_{rms} value $= (14 \pm 4)$ nm but developed heterogeneity under chromate exposure with R_{rms} value $= (35 \pm 5)$ nm.

Similar effects on cellular morphology and surface topology of exposure to chromate were also found for other gram-negative bacteria. In case of *E. coli K-12*, *S. oneidensis* MR-1 and *Pseudomonas* sp., formation of long snake-like cells due to Cr(VI) exposure has been reported (Ackerley et al. 2006; Chourey et al. 2006). It should be mentioned that cell enlargement or elongation cannot be considered as a specific response to chromate, since it has also been observed upon exposure to other stress conditions as in the case of *S. aureus* (Vijaranakul et al. 1995) exposed to high salt concentration or in the case of *S. oneidensis* (Qiu et al. 2005) exposed to UV radiation.

FTIR analysis

ATR FTIR can be exploited to efficiently study bacterial surfaces since the depth of penetration of the IR beam in this technique is limited to the thickness of the cell wall (Hind et al. 2001; Giotta et al. 2011). In the present case it was used to identify which functional group present on the cell surface appears more sensitive to chromate. In Fig. 4 are shown the spectra obtained for the case of control and 0.2 mM CrO_4^{2-} exposed cells. The intense peak due to the polypeptide backbone, called amide I, appears at 1,649 cm^{-1} and is used to normalize the two spectra at

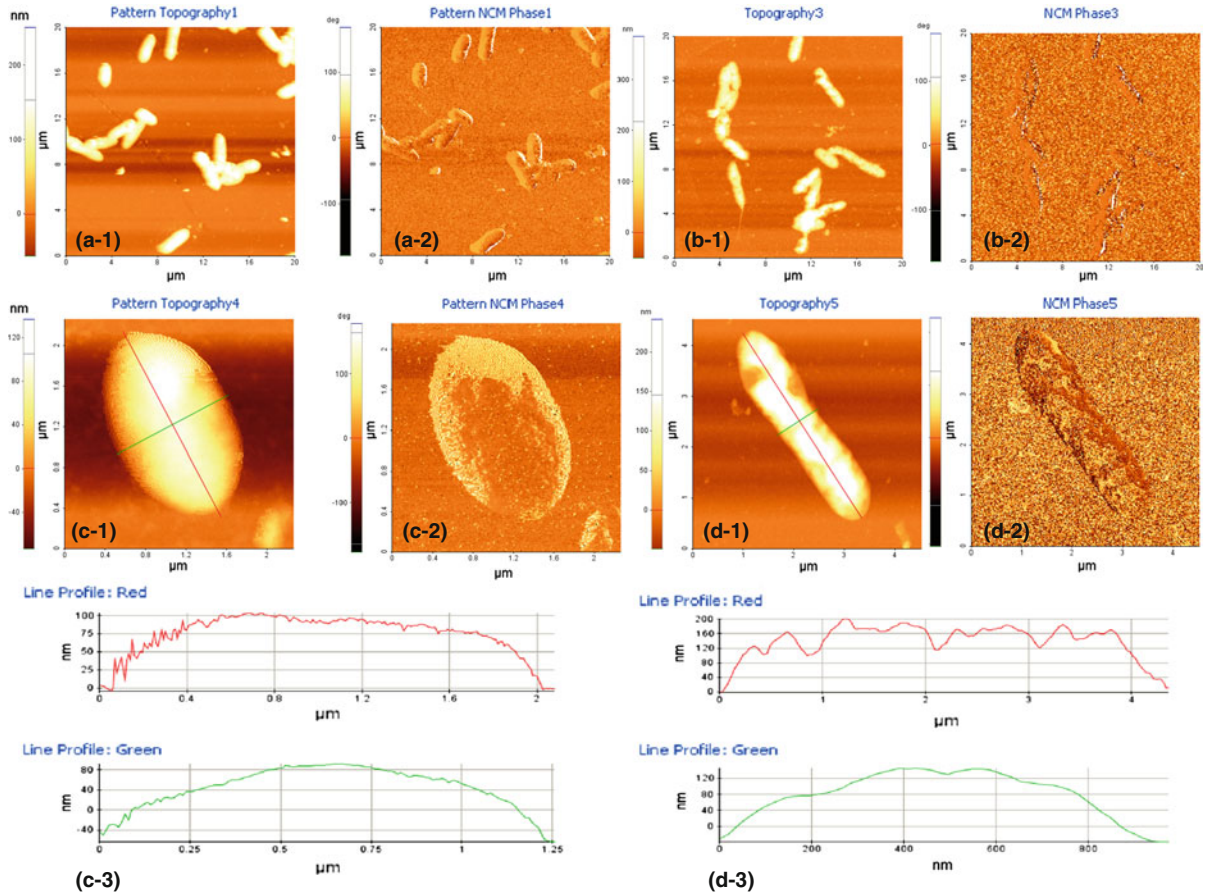

Fig. 3 Atomic force topographic image of *R. sphaeroides* cells (10^8 CFU/ml) grown in control conditions (**a-1**) and corresponding phase image (**a-2**). Atomic force topographic image of *R. sphaeroides* cells (10^8 CFU/ml) grown in 0.2 mM chromate poisoned medium (**b-1**) and corresponding phase image (**b-2**). Atomic force topographic image of a single *R. sphaeroides* cell grown in control conditions (**c-1**), corresponding phase image (**c-2**) and AFM cross section profiles (**c-3**). Atomic force topographic image of a single *R. sphaeroides* cell grown in 0.2 mM chromate poisoned medium (**d-1**) and corresponding phase image (**d-2**) and AFM cross section profiles (**d-3**). Phase images were captured simultaneously with topographic images by measuring the phase shift of the oscillating cantilever as function of tip position on the surface. Cross section profiles were measured along the two dimensions of the cell, shown as *green* and *red* lines in panels **c-1** and **d-1**. Note the different scales in the graphics. (Color figure online)

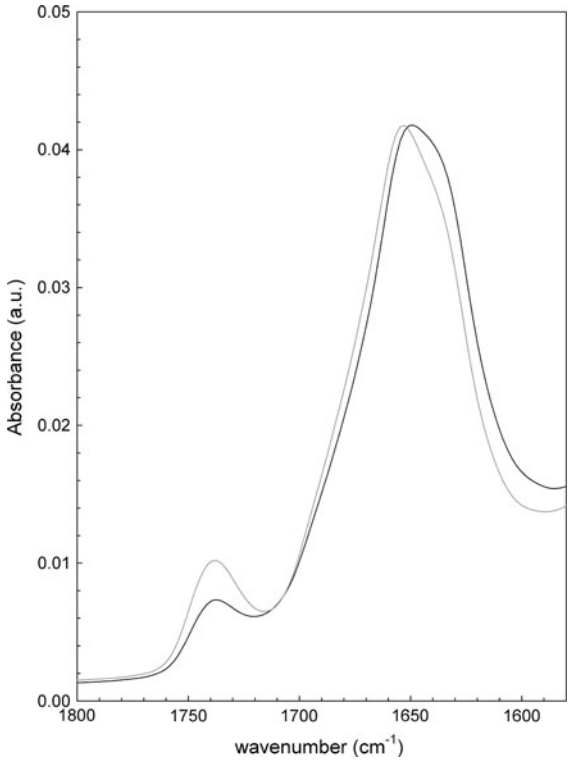

Fig. 4 ATR-FTIR spectra of *R. sphaeroides* R26 grown in control (in *black*) and 0.2 mM CrO_4^{2-} (in *light gray*) culture media. ATR-FTIR spectra were normalized against the amide I band at 1,649 cm^{-1}, the IR fingerprint of proteins, used as an internal standard for comparison between the two samples. The spectra are hence referred to the same protein concentration. The band at 1,735 cm^{-1} is ascribable to protonated carboxylic acids and ester C=O bonds, mainly present in lipids (Italiano et al. 2009) and the difference in the absorbance intensity of the band at 1,735 cm^{-1} could actually indicate that the overall concentration of fatty acids and lipids in cell envelope increases due to chromate stress. (Color figure online)

the same protein concentration. The band at 1,735 cm^{-1} is ascribable to protonated carboxylic acids and ester C=O bonds, mainly present in lipids. The intensity of this band increases in presence of chromate, indicating that in this case the cell wall contains more fatty acids than in the control.

Proteomic analysis

To understand the complexity of the mechanisms regulating the response to Cr(VI) and chromate reducing ability of *R. sphaeroides*, a proteomic investigation was performed by comparing soluble protein levels of cells exposed to chromate with those of untreated control cells. The 2DE-map in the 4–7 pH range of soluble proteins obtained from control and 0.2 mM CrO_4^{2-} media are shown in Fig. 5. Nearly 800 spots could be resolved, 30 of which showing a statistically significant difference between control and chromate proteome, with a $7 < t\text{-value} < 78$. Among these 15 were found to be up-regulated and 15 were down-regulated after exposure to CrO_4^{2-}. These spots were analyzed by MS/MS and the results were used for database searching in the currently available annotated genome of *R. sphaeroides* (http://mmg.uth.tmc.edu/sphaeroides/). A collection of relevant proteins with differential modulation is reported in Table 1 organized according to the functional categories listed by The Institute for Genomic Research reported in JCVI's Comprehensive Microbial Resource (http://cmr.jcvi.org). A more complete collection of differentially regulated proteins is given in the supporting information, Table S1. Eleven categories show altered regulation: energy metabolism (6 proteins), amino acid biosynthesis (4), fatty acid and phospholipid metabolism (2), protein fate (3), biosynthesis of cofactors, prosthetic groups and carriers (4), cell envelope (3), transport and binding proteins (1), central intermediary metabolism (2), protein synthesis (1), and transcription (1). Hypothetical proteins (1) and proteins with unknown function (2) were also found to be differentially regulated.

The metabolic response to Cr(VI) obtained by proteomic shows the up-regulation of proteins with potential antioxidant role, such as glutathione synthetase and enzymes involved in sulfur aminoacid pathway biosynthesis. The particularly high induction level of enzymes of the sulfur aminoacid pathway (cystathionine gamma-synthase, spot 4, and S-adenosylmethionine synthetase, spot 13), suggests an increased synthesis of cysteine, an efficient chromate reductant and a down-regulator of the expression of sulphate transporters which also may transport chromate (Aguilar-Barajas et al. 2011; Hesse et al. 2004). Up-regulation of proteins involved in cysteine biosynthesis has been noted in other chromate-stressed bacteria (Brown et al. 2006; Ackerley et al. 2006; Henne et al. 2009). Chromate toxicity is further marked by oxidative damage to macromolecules, and the role of cysteine in potentially minimizing cellular oxidative damage should not be overlooked (Carmel-Harel and Storz 2000). Indeed proteomics shows that CrO_4^{2-} exposure induces a strong accumulation of glutathione synthetase (spot 5), a key enzyme for the

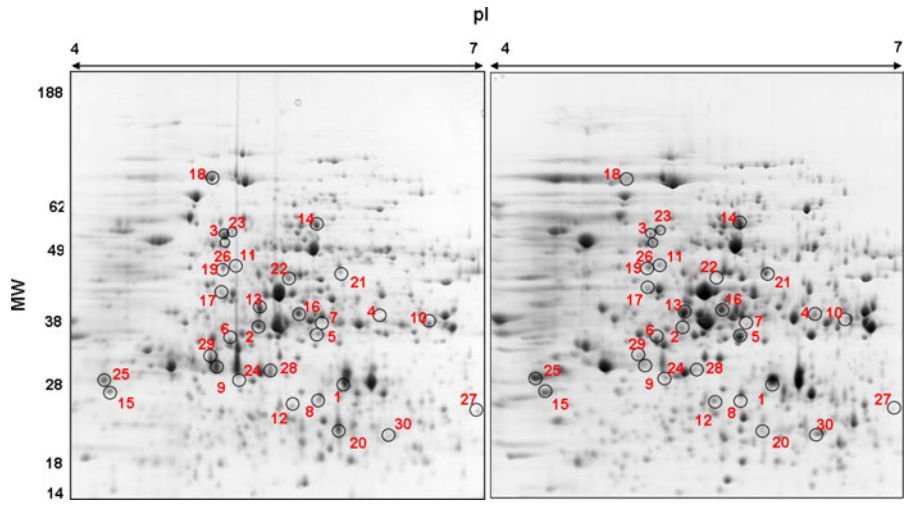

Fig. 5 Representative gels of water-soluble proteins from *R. sphaeroides* R26 grown in plain media (*left*) and in 0.2 mM CrO_4^{2-} enriched media (*right*). IEF conditions: pH 4–7 linear gradient, 70,000 Vh/tot (see "Materials and Methods" for more details). Approximately 800 distinguishable spots were obtained in both gels. Proteins showing significant ($p < 0.05$) changes in abundance are *circled*

biosynthesis of glutathione (GSH), a tripeptide with a single thiol moiety. GSH and other thiols are major cellular antioxidants (Carmel-Harel and Storz 2000) and are often involved in the response against chromate toxicity (Ackerley et al. 2006). Accordingly the normalized concentration of thiols in cells exposed to CrO_4^{2-} and measured when chromate is completely reduced, i.e. 90 h after inoculum (see Fig. 1), results increased of roughly 20 % reaching 20.3 ± 0.2 nmol of RSH per mg of proteins in cells harvested once chromate is fully reduced compared to 16.5 ± 1.2 nmol of RSH per mg of proteins in control cells. These data support the role of glutathione as reductant in chromate exposed *R. sphaeroides* cells. Glutathione was found efficient in detoxifying Cr(VI) also in *E. coli* cells (Ackerley et al. 2006). Moreover it is has been reported that absence of GSH increases CrO_4^{2-} toxicity in *E. coli* (Helbig et al. 2008). Chromate can react directly with GSH (Shi and Dalal 1988) forming adducts among which Cr(V) containing compounds that eventually form glutathione-Cr(III)-DNA adducts (Voitkun et al. 1998). Thus chromate appears to generate an overproduction of GSH which in turn, while reducing CrO_4^{2-}, produces toxic compounds detrimental to DNA integrity, therefore jeopardizing the duplication process (Salnikov et al. 2008).

Chromate stress also induces a strong increase in the expression of GroEL (spot 23), a protein belonging to the widespread class of chaperonins that are readily synthesized in prokaryotes and eukaryotes in response to a wide range of environmental stress conditions including heavy metals and oxidizing agents. In particular Dos Santos Ferreira et al. (2007) have shown that chaperonin expression level increases in *Euglena gracilis* upon exposure to chromate. Similarly a number of molecular chaperones, i.e. groES and groEL, were found to be up-regulated in *S. oneidensis* MR-1 in response to CrO_4^{2-} exposure (Chourey et al. 2006).

Bacterial cell growth occurs by the coordinated periodic alternation of morphogenic (elongation) and cell division events (Cooper 1991). Morphogenesis requires a central step involving biosynthesis and turnover of the peptidoglycan, which functions as principal stress-bearing and shape maintenance component of the cell wall. Chromate exposure of *R. sphaeroides* cells provokes an eightfold decrease of the level of two enzymes involved in the cell wall biosynthesis, namely dTDP-glucose 4,6-dehydratase (belonging also to the pathway of the dTDP-L-rhamnose biosynthesis, spot 10) and D-alanine-D-alanine ligase (catalyzing an early step in peptidoglycan biosynthesis, spot 9). Such down-regulation is consistent with the morphological changes in cell structure seen by AFM. Indeed the presence of a lower quantity of cell wall components would require less cell wall material to assemble a larger ellipsoid than many smaller ones. The involvement of the cell wall in the reduction of chromate would also agree with the increase in the surface roughness of the cell as found in AFM measurements as a rougher surface would increase the overall area making this reaction more efficient.

Table 1 MS/MS identification of *R. sphaeroides* polypeptides resolved by 2D-PAGE (Fig. 5)

Spot number	Protein name	NCBI accession number	EC-number	Number of peptides identified by MS/MS	Mascot score	% Sequence coverage	Mr, kDa theor.	pI predict.	*t*-value	Relative fold difference chromate/control
Aminoacid biosynthesis										
S4	Cystathionine gamma-synthase	gil77463474	–	2	92	33	42.1	5.84	13.66	686
Biosynthesis of cofactors, prosthetic groups, and carriers										
S5	Glutathione synthetase	gil77462359	6.3.2.3	5	282	15	35.4	5.60	36.22	6.9×10^3
Cell envelope										
S9	D-alanine-D-alanine ligase	gil77462663	6.3.2.4	1	80	5	33.2	4.98	29.89	0.13
S10	dTDP-glucose 4,6-dehydratase	gil125654613	4.2.1.46	13	679	46	38.2	5.95	7.54	0.12
Central intermediary metabolism										
S13	S-adenosylmethionine synthetase	gil77465596	2.5.1.6	24	1415	71	42.8	5.18	14.21	5.8
Protein fate										
S23	Chaperonin GroEL	gil77462862	3.6.4.9	7	409	27	57.9	5.00	78.03	220.0
S24	Signal recognition particle-docking protein FtsY	gil77462389	3.6.5.4	3	370	26	30.5	5.06	13.25	81.0

The *t* test statistic is based on the difference between the % volume mean values (X) of the two classes, normalized by the standard deviations (s). The proteins identified were organized according to the functional category assignments given in JCVI's Comprehensive Microbial Resource (http://cmr.jcvi.org)

Interestingly, an 80-fold increase of the signal recognition particle-docking protein FtsY (spot 24) was found in CrO_4^{2-} cells. *ftsY* is an essential gene that, in *E. coli*, is located in an operon named *fts* (temperature-sensitive filamentation) encoding for proteins involved in septum formation and cell division. Cells defective in the expression of the proteins FstI, FstL, and FstQ give rise to abnormal morphologies characterized by long, aseptate filaments that eventually lise (Guzman et al. 1997). The up-regulation of FtsY appears to contradict the above mentioned reduced ability of *R. sphaeroides* to undergo duplication but this protein however is not directly involved in cell-division, rather its apparent function is to recognize N-terminal sequences of newly synthesized polypeptides at the ribosome and appears more closely related to protein synthesis than to cell duplication (Guzman et al. 1997).

The response to chromate stress exposure of *R. sphaeroides* growing under photosynthetic conditions includes several modifications in the soluble proteome and in cell morphology. Notwithstanding these relevant changes, it was proven to completely reduce chromate at 0.2 mM by involving both the cytoplasmic and, to a lesser extent, the cell wall portions of the bacterium. *R. sphaeroides* hence shows potential applications in environmental issues related to soil or water detoxification to be tested in field experiments.

Acknowledgments The authors wish to thank Mr. Giovanni Lasorella for his help with AFM measurements. Paola Nitti, Giacomo Colasuonno and Francesco Di Paolo are gratefully acknowledged. Livia Giotta is thanked for suggestions in the interpretation of ATR-FTIR measurements. Support for this work was obtained by the Italian Ministry of Research Education and Education (Prin 2009) and by COST Action CM0902 *Molecular machinery for ion translocation across the membrane.*

References

Ackerley DF, Gonzalez CF, Keyhan M, Blake R, Matin A (2004) Mechanism of chromate reduction by the *Escherichia coli* protein, NfsA, and the role of different chromate reductases in minimizing oxidative stress during chromate reduction. Environ Microbiol 6(8):851–860

Ackerley DF, Barak Y, Lynch SV, Curtin J, Matin A (2006) Effect of chromate stress on *Escherichia coli* K-12. J Bacteriol 188(9):3371–3381

Aguilar-Barajas E, Diaz-Perez C, Ramirez-Diaz MI, Riveros-Rosas H, Cervantes C (2011) Bacterial transport of sulfate, molybdate, and related oxyanions. Biometals 24(4): 687–707. doi:10.1007/s10534-011-9421-x

Barceloux DG (1999) Chromium. J Toxicol Clin Toxicol 37(2):173–194

Borsetti F, Toninello A, Zannoni D (2003) Tellurite uptake by cells of the facultative phototroph *Rhodobacter capsulatus* is a delta pH-dependent process. FEBS Lett 554:315–318

Brown SD, Thompson MR, Verberkmoes NC, Chourey K, Shah M, Zhou J, Hettich RL, Thompson DK (2006) Molecular dynamics of the *Shewanella oneidensis* response to chromate stress. Mol Cell Proteomics 5(6):1054–1071

Buccolieri A, Italiano F, Dell'Atti A, Buccolieri G, Giotta L, Agostiano A, Milano F, Trotta M (2006) Testing the photosynthetic bacterium *Rhodobacter sphaeroides* as heavy metal removal tool. Ann Chim 96(3–4):195–203

Carmel-Harel O, Storz G (2000) Roles of the glutathione- and thioredoxin-dependent reduction systems in the *Escherichia coli* and *Saccharomyces cerevisiae* responses to oxidative stress. Annu Rev Microbiol 54:439–461

Cervantes C, Campos-Garcia J, Devars S, Gutierrez-Corona F, Loza-Tavera H, Torres-Guzman JC, Moreno-Sanchez R (2001) Interactions of chromium with microorganisms and plants. FEMS Microbiol Rev 25(3):335–347

Cheung KH, Gu J-D (2007) Mechanism of hexavalent chromium detoxification by microorganisms and bioremediation application potential: a review. Int Biodet Biodegrad 59(1):8–15

Chourey K, Thompson MR, Morrell-Falvey J, Verberkmoes NC, Brown SD, Shah M, Zhou J, Doktycz M, Hettich RL, Thompson DK (2006) Global molecular and morphological effects of 24-hour chromium(VI) exposure on *Shewanella oneidensis* MR-1. Appl Environ Microbiol 72(9): 6331–6344

Codd R, Irwin JA, Lay PA (2003) Sialoglycoprotein and carbohydrate complexes in chromium toxicity. Curr Opin Chem Biol 7(2):213–219

Cooper S (1991) Bacterial growth and division. Academic Press, Inc., San Diego

Dos Santos Ferreira V, Rocchetta I, Conforti V, Bench S, Feldman R, Levin MJ (2007) Gene expression patterns in *Euglena gracilis*: insights into the cellular response to environmental stress. Gene 389(2):136–145

Giotta L, Agostiano A, Italiano F, Milano F, Trotta M (2006) Heavy metal ion influence on the photosynthetic growth of *Rhodobacter sphaeroides*. Chemosphere 62(9):1490–1499

Giotta L, Mastrogiacomo D, Italiano F, Milano F, Agostiano A, Nagy K, Valli L, Trotta M (2011) Reversible binding of metal ions onto bacterial layers revealed by protonation-induced ATR-FTIR difference spectroscopy. Langmuir 27(7):3762–3773. doi:10.1021/la104868m

Guzman LM, Weiss DS, Beckwith J (1997) Domain-swapping analysis of FtsI, FtsL, and FtsQ, bitopic membrane proteins essential for cell division in *Escherichia coli*. J Bacteriol 179(16):5094–5103

Helbig K, Bleuel C, Krauss GJ, Nies DH (2008) Glutathione and transition-metal homeostasis in *Escherichia coli*. J Bacteriol 190(15):5431–5438

Henne KL, Turse JE, Nicora CD, Lipton MS, Tollaksen SL, Lindberg C, Babnigg G, Giometti CS, Nakatsu CH, Thompson DK, Konopka AE (2009) Global proteomic

analysis of the chromate response in *Arthrobacter* sp. strain FB24. J Proteome Res 8(4):1704–1716

Hesse H, Nikiforova V, Gakiere B, Hoefgen R (2004) Molecular analysis and control of cysteine biosynthesis: integration of nitrogen and sulphur metabolism. J Exp Bot 55(401): 1283–1292

Hind AR, Bhargava SK, McKinnon A (2001) At the solid/liquid interface: FTIR/ATR: the tool of choice. Adv Colloid Interface Sci 93(1–3):91–114

Italiano F, Buccolieri A, Giotta L, Agostiano A, Valli L, Milano F, Trotta M (2009) Response of the carotenoidless mutant *Rhodobacter sphaeroides* growing cells to cobalt and nickel exposure. Int Biodeter Biodegrad 63(7):948–957

Italiano F, D'Amici GM, Rinalducci S, De Leo F, Zolla L, Gallerani R, Trotta M, Ceci LR (2011) The photosynthetic membrane proteome of *Rhodobacter sphaeroides* R-26.1 exposed to cobalt. Res Microbiol 162(5):520–527

Katz SA, Salem H (1993) The toxicology of chromium with respect to its chemical speciation: a review. J Appl Toxicol 13:217–224

Kiley PJ, Kaplan S (1988) Molecular genetics of photosynthetic membrane biosynthesis in *Rhodobacter sphaeroides*. Microbiol Rev 52(1):50–69

Lovley DR, Phillips EJ (1994) Reduction of chromate by *Desulfovibrio vulgaris* and its c(3) cytochrome. Appl Environ Microbiol 60(2):726–728

McLean JS, Beveridge TJ, Phipps D (2000) Isolation and characterization of a chromium-reducing bacterium from a chromated copper arsenate-contaminated site. Environ Microbiol 2(6):611–619

Morais PV, Branco R, Francisco R (2011) Chromium resistance strategies and toxicity: what makes *Ochrobactrum tritici* 5bvl1 a strain highly resistant. Biometals 24(3):401–410. doi:10.1007/s10534-011-9446-1

Myers CR, Carstens BP, Antoline WE, Myers JM (2002) Chromium (VI) reductase activity is associated with the cytoplasmic membrane of anaerobically grown *Shewanella putrefaciens* MR-1. J Appl Microbiol 88:98–106

Park CH, Keyhan M, Wielinga B, Fendorf S, Matin A (2000) Purification to homogeneity and characterization of a novel *Pseudomonas putida* chromate reductase. Appl Environ Microbiol 66(5):1788–1795

Pimentel BE, Moreno-Sanchez R, Cervantes C (2002) Efflux of chromate by *Pseudomonas aeruginosa* cells expressing the ChrA protein. FEMS Microbiol Lett 212(2):249–254

Pisani F, Italiano F, de Leo F, Gallerani R, Rinalducci S, Zolla L, Agostiano A, Ceci LR, Trotta M (2009) Soluble proteome investigation of cobalt effect on the carotenoidless mutant of *Rhodobacter sphaeroides*. J Appl Microbiol 106(1): 338–349

Plaper A, Jenko-Brinovec S, Premzl A, Kos J, Raspor P (2002) Genotoxicity of trivalent chromium in bacterial cells. Possible effects on DNA topology. Chem Res Toxicol 15(7): 943–949

Qiu X, Sundin GW, Wu L, Zhou J, Tiedje JM (2005) Comparative analysis of differentially expressed genes in *Shewanella oneidensis* MR-1 following exposure to UVC, UVB, and UVA radiation. J Bacteriol 187:3556–3564

Ramirez-Diaz MI, Diaz-Perez C, Vargas E, Riveros-Rosas H, Campos-Garcia J, Cervantes C (2008) Mechanisms of bacterial resistance to chromium compounds. Biometals 21(3):321–332

Salnikov VV, Ageeva MV, Gorshkova TA (2008) Homofusion of Golgi secretory vesicles in flax phloem fibers during formation of the gelatinous secondary cell wall. Protoplasma 233(3–4):269–273. doi:10.1007/s00709-008-0011-x

Schaer-Zammaretti P, Ubbink J (2003) Imaging of lactic acid bacteria with AFM-elasticity and adhesion maps and their relationship to biological and structural data. Ultramicroscopy 97(1–4):199–208

Schultz JE, Weaver PF (1982) Fermentation and anaerobic respiration by *Rhodospirillum rubrum* and *Rhodopseudomonas capsulata*. J Bacteriol 149(1):181–190

Shi XL, Dalal NS (1988) On the mechanism of the chromate reduction by glutathione: ESR evidence for the glutathionyl radical and an isolable Cr(V) intermediate. Biochem Biophys Res Commun 156(1):137–142

Sistrom WR, Griffiths M, Stanier RY (1956) The biology of photosynthetic bacterium which lacks colored carotenoids. J Cell Physiol 48(3):473–515

Smith PK, Krohn RI, Hermanson GT, Mallia AK, Gartner FH, Provenzano MD, Fujimoto EK, Goeke NM, Olson BJ, Klenk DC (1985) Measurement of protein using bicinchoninic acid. Anal Biochem 150(1):76–85

Stearns DM, Kennedy LJ, Coutney KD, Giangrande PH, Phieffer LS, Wetterhahn KE (1995) Reduction of chromium(VI) by ascorbate leads to chromium-DNA binding and DNA strand breaks in vitro. Biochemistry-US 34:910–919

Suzuki T, Miyata N, Horitsu H, Kawai K, Takamizawa K, Tai Y, Okazaki M (1992) NAD(P) H-dependent chromium (VI) reductase of *Pseudomonas ambigua* G-1: a Cr(V) intermediate is formed during the reduction of Cr(VI) to Cr(III). J Bacteriol 174(16):5340–5345

Turner RJ, Weiner JH, Taylor DE (1999) Tellurite-mediated thiol oxidation in *Escherichia coli*. Microbiology 145(Pt 9): 2549–2557

Vijaranakul U, Nadakavukaren MJ, de Jonge BLM, Wilkinson BJ, Jayaswal RK (1995) Increased cell size and shortened peptidoglycan interpeptide bridge of NaCl-stressed *Staphylococcus aureus* and their reversal by glycine betaine. J Bacteriol 177:5116–5121

Voitkun V, Zhitkovich A, Costa M (1998) Cr(III)-mediated crosslinks of glutathione or amino acids to the DNA phosphate backbone are mutagenic in human cells. Nucleic Acids Res 26(8):2024–2030

Wang PC, Mori T, Toda K, Ohtake H (1990) Membrane-associated chromate reductase activity from *Enterobacter cloacae*. J Bacteriol 172(3):1670–1672